UNIVERSIDADE DE SÃO PAULO

INSTITUTO DE FÍSICA
CAIXA POSTAL 20516
01498 - SÃO PAULO - SP
BRASIL

PUBLICAÇÕES

IFUSP/P-795

ISOTHERMAL ANNEALING KINETICS OF X-IRRADIATED PYRENE BY EPR

C.S.M. Partiti, W.M. Pontuschka, A. Fazzio and A. Piccini
Instituto de Física, Universidade de São Paulo

Julho/1989

ISOTHERMAL ANNEALING KINETICS OF X–IRRADIATED PYRENE BY EPR

C.S.M. PARTITI, W.M. PONTUSCHKA, A. FAZZIO

AND

A. PICCINI

Instituto de Física, Universidade de São Paulo,
C.P. 20516, 01498 São Paulo, SP, Brazil

Copies submitted: 3

Manuscript pages: 12

Figures: 7

Tables: 1

ISOTHERMAL ANNEALING KINETICS OF X–IRRADIATED PYRENE BY EPR

Carmen Silvia de Moya Partiti

Instituto de Física, Universidade de São Paulo,
C.P. 20.516, 01498 São Paulo, SP, Brazil

The annealing behavior of X–irradiated stable free radicals found in pyrene ($C_{16}H_{10}$) single crystals was studied by EPR. Two processes of thermal decay kinetics were found, both with the same activation energy: (1.9 ± 0.1)eV.

INTRODUCTION

EPR and optical absorption of single crystals irradiated by X–rays, electrons or γ–rays of aromatic compounds: benzene (1–6), naphtalene (4,6–11), anthracene (8,12), toluene (1), chrysene (13), phenanthrene (14) and pyrene (15) have revealed stable radicals at room temperature.

Kawakubo (15) explained the observed EPR spectra of pyrene as contributions from two kinds of hydrogen adducts 2–H_2 and 3–H_2 pyrene (additional hydrogen at positions 2 and 3, respectively, as seen in figure 1). He used MacLachlan's method (16,17) to calculate

INSERT FIGURE 1

spin densities and inferred also that the central line of the triplet relative to the other lines was larger than 1:2:1 and suggested a presence of an additional singlet of hydrogen abstraction pyrene radicals which do not recombine even at room temperature. But he did not calculate the splitting of these radicals and so this problem has not yet been solved. We calculated the splitting of 2–pyrenil (hydrogen abstraction atom at position 2), and 3–pyrenil (hydrogen abstraction atom at position 3) using the INDO/2 approximation (18) in this work.

Though several studies of irradiated aromatic compounds have been performed at 77K, similar work with pyrene is not feasible at low temperatures, because the crystal usually shatters upon cooling below 120K, a phenomenon coincident with a phase transition (19–21). It appeared that a thermal annealing study of X–irradiated pyrene single crystals, by EPR, above room temperature could provide a clear identification of the radicals produced. The thermal annealing behavior of these radicals in pyrene was therefore studied, by EPR, between 373K and 413K, in this work.

EXPERIMENTAL

Pyrene single crystals, grown by the Bridgman method, were kindly furnished by Dr. William B. Whitten.

The crystals of $2 \times 2 \times 8$ mm were isotropically X–irradiated at room temperature, from a chromium target to a dose of the order of about 10^6 rad. A new X–irradiated sample was used to each isothermal annealing.

The crystal orientation was found by identifying the ab plane (easy cleavage) and determining the direction of birrefringence.

The crystal was oriented with the b–axis perpendicular to the magnetic field and θ is the angle between the a–axis and the external magnetic field direction (15).

The EPR measurements were made with a homodine X–band spectrometer at temperatures ranging from room temperature to 413K. The temperature was measurd, within ± 1K, with chromel–alumel thermocouple located 1 mm above the sample in the EPR cavity and controlled by a regulated current through and electric heater in a nitrogen gas flow. The system was controlled by a Varian V4540 Variable Temperature Controller unit.

RESULTS AND DISCUSSION

Spectra measured at room temperature, with θ equal to 0°, 30° and 150° are shown in figures 2, 3 and 4. All the spectra exhibit a broad triplet of the hydrogen addition

INSERT FIGURES 2, 3 AND 4

radical. The intensity of central line is greater than the ratio 1:2:1. The figure 3 only presents the triplet and the others exhibit structures of 2.10^{-4} T and 5.10^{-4} T splittings. Our annealing measurements performed by EPR are in agreement with Kawakubo's assumption (15) of the presence of hydrogen addition pyrene radicals. Also his calculations were reproduced by us using the reported spin densities (15) in order to check

unambiguously the nature of hyperfine couplings as shown by the spectra attributed to 2–H_2 and 3–H_2 radicals, as mentioned above.

Using the semiempirical self–consistent method, Intermediate–Neglect–of–Differential–Overlap (INDO/2) (18) which includes one–center exchange integrals, we calculated the electronic structure of pyrene, 2–pyrenil radical (due to H abstraction at position 2), 3–pyrenil and 4–pyrenil radical. In this approach the unpaired spin density ρ^{spin} is written as

$$\rho^{spin}(\vec{r}) = \sum_{\mu\nu} \rho_{\mu\nu}^{spin} \chi_\mu^*(\vec{r}) \chi_\nu(\vec{r})$$

with

$$\rho_{\mu\nu}^{spin} = p_{\mu\nu}^{\alpha} - p_{\mu\nu}^{\beta} \quad \text{and}$$

$$p_{\mu\nu}^{\alpha(\beta)} = \sum_i C_{\mu i}^{\alpha(\beta)} C_{\nu i}^{\alpha(\beta)}, \quad \text{where the sum is over all occupied orbitals}$$

$\varphi_i = \sum_\mu C_{i\mu} \chi_\mu$. The atomic orbitals ($\chi_\mu$) utilized are Slater type. In table I we present the results for the isotropic hyperfine coupling constant, $a_N = Q\,\rho^{spin}$ with $Q = 0{,}0508$ T (14). The doublets with splittings of 19.9 and 21.1 10^{-4} T of the 2–pyrenil radical and 3–pyrenil radical are not resolved in the central line of the triplet, yielding an enhanced central line.

Therefore, we suppose that the EPR spectra of pyrene, at room temperature, are composed of hydrogen addition and abstraction radicals. A similar work with phenanthrene (14) reported the same conclusion.

Several X–irradiated samples were measured with $\theta = 150°$ (see figure 4) at different temperatures namely 373, 383, 393, 403 and 413K. While the sample was maintained at constant temperature, the measurements were taken at regular intervals of time. The highest temperature of measurements was limited by the melting point of pyrene at 423K (22). The peak to peak amplitude of the EPR triplet central line was used as a measure of the concentration, since the line width did not change with temperature.

Our experimental results for isothermal decay at 373K are shown in figure 5. The

INSERT FIGURE 5

graphs obtained at 383K and 393K are analogous. So, except for the isothermal decay at 403K and 413K, that showed one straight line, the graphs at 373K, 383K and 393K could be analysed as a sum of two first order processes. The final experimental points were adjusted by first order processes. The final experimental points were adjusted by a least squares method in the Log I × time graph, yielding the first straight line. The second one was obtained by subtracting the first line from the initial experimental points and adjusting again, resulting in the second straight line as seen in figure 5. Therefore, the decay kinetics can be explained as a sum of two frist order processes (23). In figure 6, two

INSERT FIGURE 6

parallel straight lines are shown in the Arrhenius plot Log r × 1/T . They yield the same value of activation energy (1.9 × 0.1)eV, but different pre–exponential factors, 1.3×10^{20} sec^{-1} and 7.6×10^{21} sec^{-1}.

After the initial fast decay, corresponding to the first experimental points, namely: 350 minutes at 373K, 150 minutes at 383K and 20 minutes at 393K (see figure 5), the remaining EPR spectra exhibit a triplet related to 2–H_2 pyrene and 3–H_2 pyrene radicals and the hyperfine structure of these radicals. So, the initial process can be attributed to the annealing of the hydrogen abstraction radicals and the subsequent one to the hydrogen addition radicals. In figure 7, it is shown a spectrum after the thermal annealing.

INSERT FIGURE 7

The above results led us to suggest that the hydrogen abstraction radicals were

annealed before the addition radicals, with the same value of activation energy (1.9 × 0.1)eV.

Thus, possible reactions which are consistent with the radicals formation are:

$$C_{16}H_{10} + X_{rays} \longrightarrow C_{16}H_9 + H \quad [1]$$

$$C_{16}H_{10} + H \longrightarrow C_{16}H_{11} \quad [2]$$

and on annealing,

$$C_{16}H_{11} \longrightarrow C_{16}H_{10} + H \quad [3]$$

$$C_{16}H_9 + H \longrightarrow C_{16}H_{10} \quad [4]$$

Though the hydrogen abstraction radicals anneal first, the two last reactions above are dependent on each other and so the coincidence of activation energy is acceptable. EPR experiments indicate no radicals other than hydrogen addition and abstraction radicals. Although it was not directly observed, we suggest that the reaction

$$C_{16}H_9 + C_{16}H_{10} \longrightarrow (C_{16}H_9)_2 + H \quad [5]$$

might occur, in agreement with Chong and Iton on naphtalene (10). This leads to the conclusion that some hydrogen abstraction radicals were converted into diamagnetic molecules.

The hydrogen abstraction radicals are known to be more reactive than hydrogen addition radicals (10) in agreement with our results.

CONCLUSIONS

The EPR spectra of X–irradiated pyrene single crystals at room temperature exhibit hydrogen abstraction and addition radicals. The hydrogen abstraction radicals anneal before hydrogen addition radicals, with the same activation energy but different pre–exponential factors.

ACKNOWLEDGMENTS

We are grateful to Dr. William B. Whitten for providing the pyrene crystals and Dr. Hercílio R. Rechemberg for discussions and suggestions. This work was supoported by FAPESP and CAPES.

REFERENCES

1. S. Ohnishi, T. Tanei and I. Nitta, ESR Study of Free Radicals Produced by Irradiation in Benzene and Its Derivations, J. Chem. Phys. **37**, 2402 (1962).
2. R.W. Fessenden and R.H. Schuler, ESR Spectrum of the Cyclohexadienyl Radical, J. Chem. Phys. **38**, 773 (1963).
3. R.B. Ingalls and D. Kivelson, Analysis of ESR Spectra Observed in Irradiated Aromatic Systems, J. Chem. Phys. **38**, 1907 (1963).
4. J.A. Leone and W.S. Koski, The Reaction of Hydrogen Atoms with Some Conjugated Ring Systems at 77°K, J. Am. Chem. Soc. **88**, 656 (1966).
5. D. Campbell, M.C.R. Symons and G.S.P. Verma, Unstable Intermediates. Part LXIV. A Comparison between the Reactions of Atomic Hydrogen with Some Substituted Benzenes and those Induced by γ–Irradiation, J. Chem. Soc. **1969**, 2480 (1969).
6. T. Shida and I. Hanazaki, Electronic Structures and Electronic Absorption Spectra of Cyclohexadienyl and Related Radicals Produced by γ–Irradiation, Bull. Chem. Soc. Japan, **43**, 646 (1970).
7. T. Okubo, N. Itoh and T. Suita, Radiation Damage in Naphtalene Single Crystals, J. Phys. Soc. Japan **24**, 1179 (1968).
8. Y. Akasaka, K. Masuda and S. Namba, Paramagnetic Defects Induced in Naphtalene and Anthracene Single Crystals by Neutron Irradiation at Low Temperature, J. Phys. Soc. Japan **30**, 1686 (1971).
9. N. Itoh and T. Okubo, An ESR Study of Hydronaphthyl Radical in Naphthalene Single Crystals, Mol. Cryst. and Liq. Cryst. **17**, 303 (1972).
10. T. Chong and N. Itoh, Electronic Paramagnetic Resonance and Optical Absorption Studies of Radiation–Induced Radicals in Naphtalene Single Crystals, J. Phys. Soc. Japan **35**, 518 (1973).
11. Y. Akasaka, K. Murakami, K. Masuda and S. Namba, Optical Absorption Measurements of α–Hydronaphthyl Radical produced in Naphthalene by Electron Beam Irradiation and Hydrogen Atom Bombardment, Mol. Cryst. and Liq. Cryst. **15**, 37 (1971).
12. T. Chong and N. Itoh, Radiation–Induced Radicals in Anthracene Single Crystals, Mol. Cryst. and Liq. Cryst. **36**, 99 (1976).
13. R.W. Jennings and L.K. Wilson, Paramagnetic Centers in X–Irradiated Chrysene Single Crystals, Mol. Cryst. and Liq. Cryst. **17**, 315 (1972).
14. T. Kawakubo, Optical and EPR Studies of Radiation–Induced Radicals in Phenanthrene Single Crystals, Mol. Cryst. and Liq. Cryst. **62**, 41 (1980).
15. T. Kawakubo, EPR and Optical Absorption Studies of γ–Irradiated Pyrene Single Crystals, Mol. Cryst. and Liq. Cryst. **46**, 11 (1978).
16. A.D. McLachlan, Hyperconjugation in the Electron Resonance Spectra of Free Radicals, Mol. Phys. **1**, 223 (1958).
17. A.D. McLachlan, Self–Consistent Field Theory of the Electron Spin Distribution in π–Electron Radicals, Mol. Phys. **3**, 233 (1960).
18. J.A. Pople, D.L. Beveridge and P.A. Dobosh, Approximate Self–Consistent Molecular–Orbital Theory. V. Intermediate Neglect of Differential Overlap, J. Chem. Phys. **47**, 2026 (1967).
19. W. Jones, S. Ramdas and J.M. Thomas, Novel Approach to the Determination of the Crystal Structures of Organic Molecular Crystals: Low Temperature Form of Pyrene, Chem. Phys. Letters **54**, 490 (1978).
20. A. Matsui, K. Tomioka and T. Tomotika, Structural Phase Transition in Pyrene – How does it occur?, Solid St. Commun. **25**, 237 (1978).
21. J.C.A. Boeyens, Rotational Disorder in Crystalline Pyrene as a Model of Layered Aromatic Structures, J. Chem. Phys. **83**, 2368 (1985).

22. Handbook of Chemistry and Physics 1960–1961, Chemical Rubber Publishing Co.
23. J.A. Partridge and C.E. May, EPR Study of Isothermal Annealing Kinetics of the F Center in KCl, Phys. Lett. **30A**, 248 (1969).

TABLE I

The isotropic hyperfine coupling constant (10^{-4} T) obtained using INDO, for the 3 types of abstraction pyrenil radicals.

Hydrogen	2–Pyrenil	3–Pyrenil	4–Pyrenil
4	——	21,1	——
10	——	——	17,5
1	19,9	——	——
2	——	——	11,8

FIGURE CAPTIONS

FIG. 1 – Carbon positions at pyrene molecule.

FIG. 2 – EPR spectra of pyrene, $\theta = 0°$, θ denotes the angle between magnetic field and a–axis.

FIG. 3 – EPR spectra of pyrene, $\theta = 30°$, θ denotes the angle between magnetic field and a–axis.

FIG. 4 – EPR spectra of pyrene, $\theta = 150°$, θ denotes the angle between magnetic field and a–axis.

FIG. 5 – Isothermal annealing of X–irradiated pyrene EPR signal intensity at 373K. The solid lines were adjusted as first order processes, the sum of which fit the experimental points.

FIG. 6 – Arrhenius plot of both first order processes obtained from the isothermal annealing shown in Figure 5.

FIG. 7 – EPR spectra of pyrene $\theta = 150°$, after annealing at 373K.

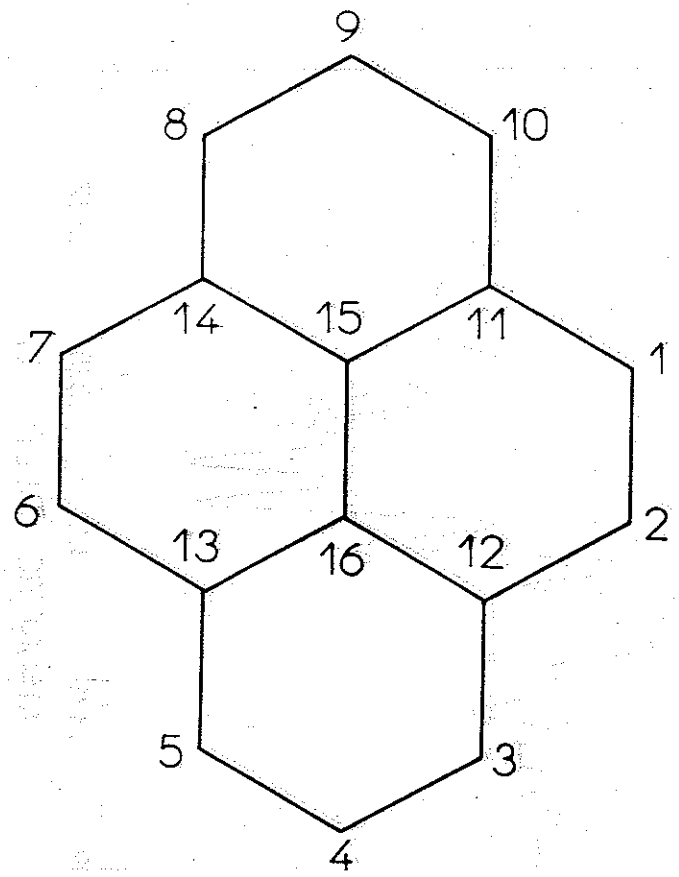

Figure 1

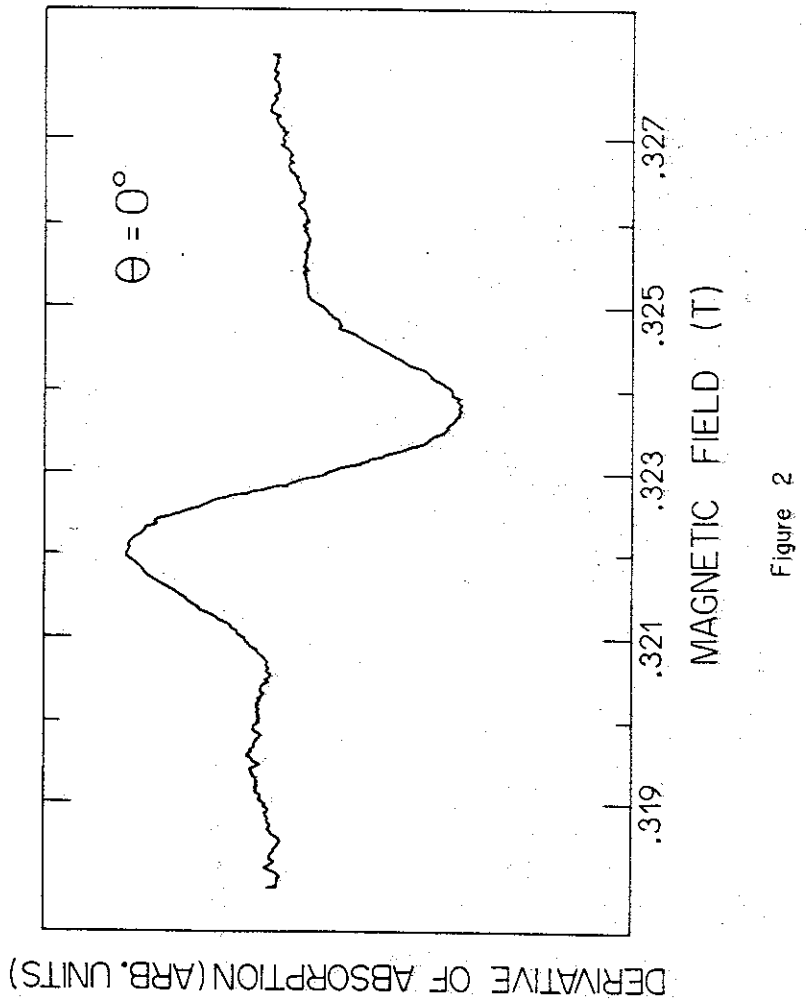

Figure 2

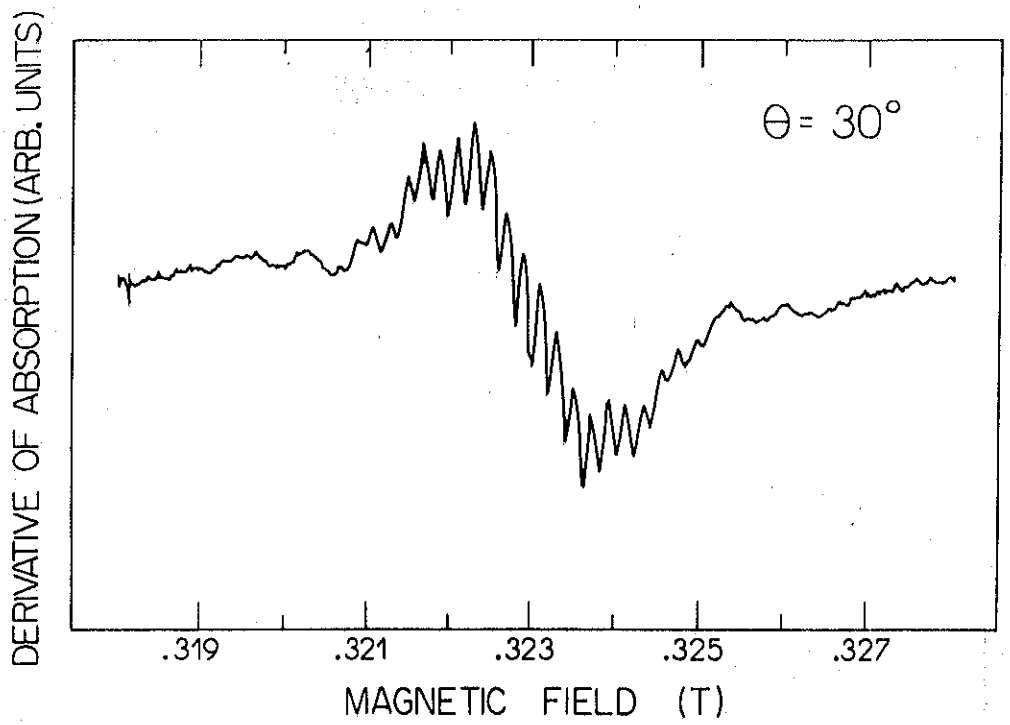

Figure 3

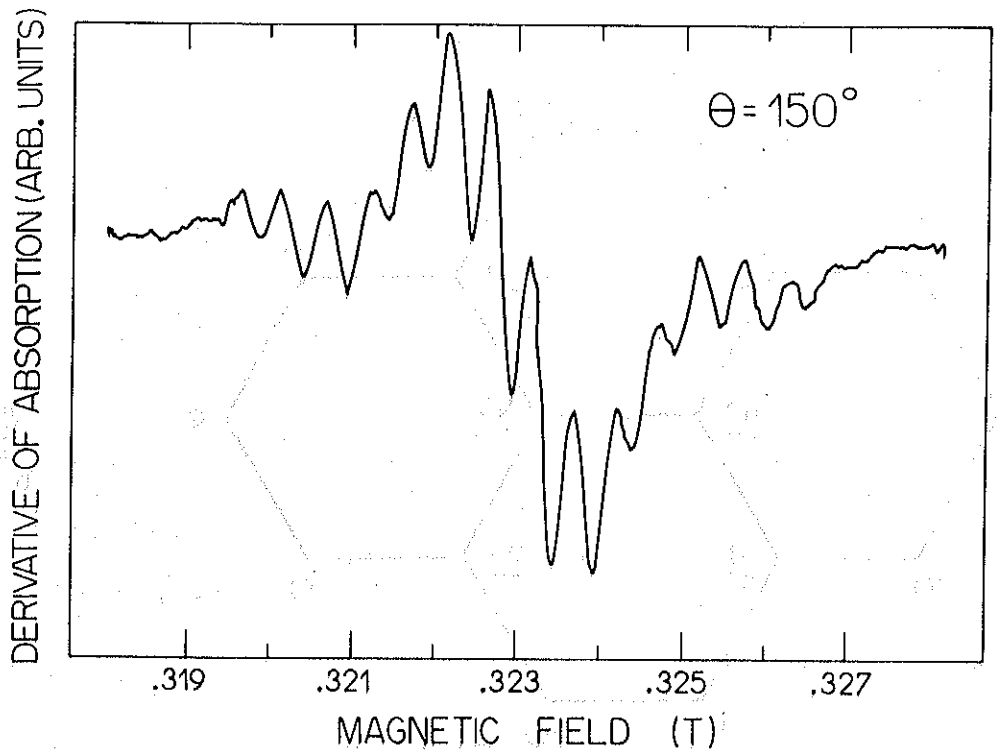

Figure 4

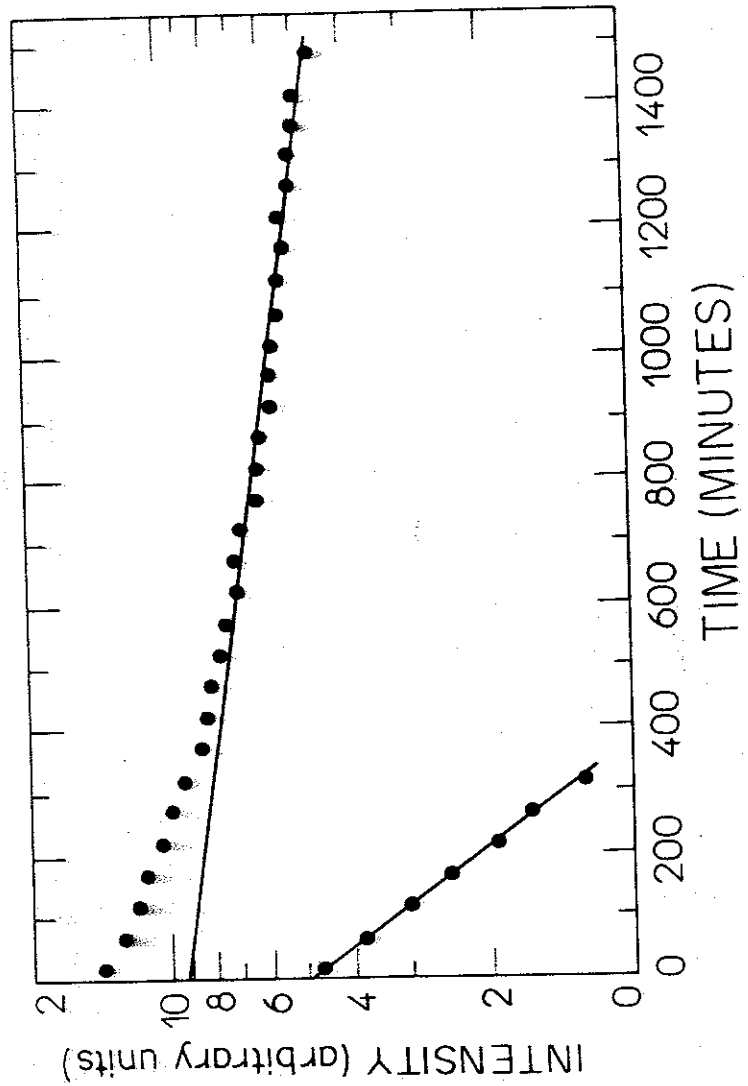

Figure 5

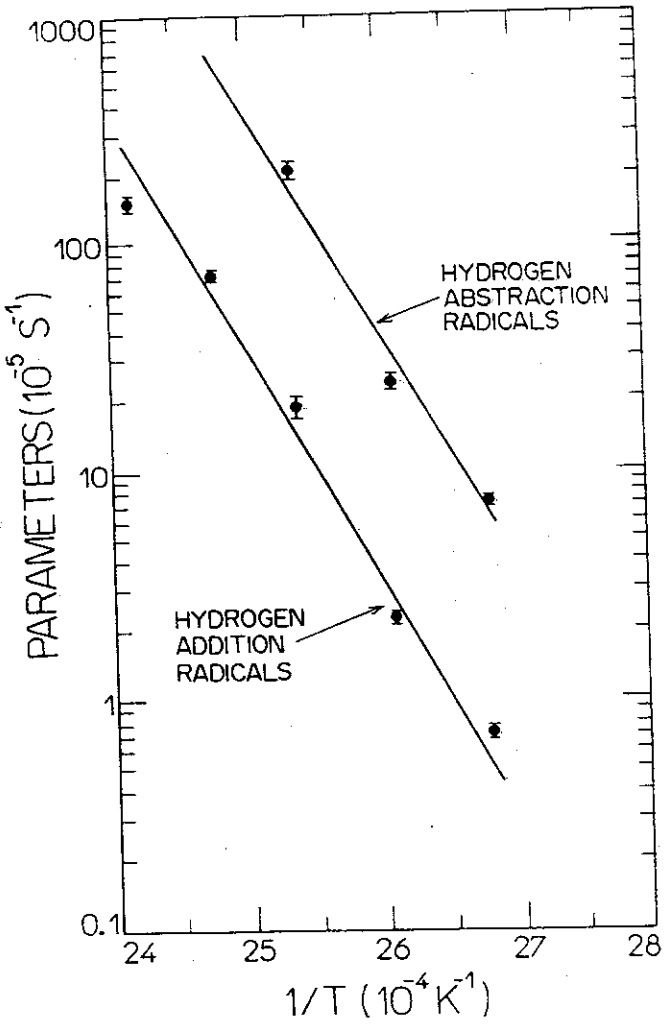

Figure 6

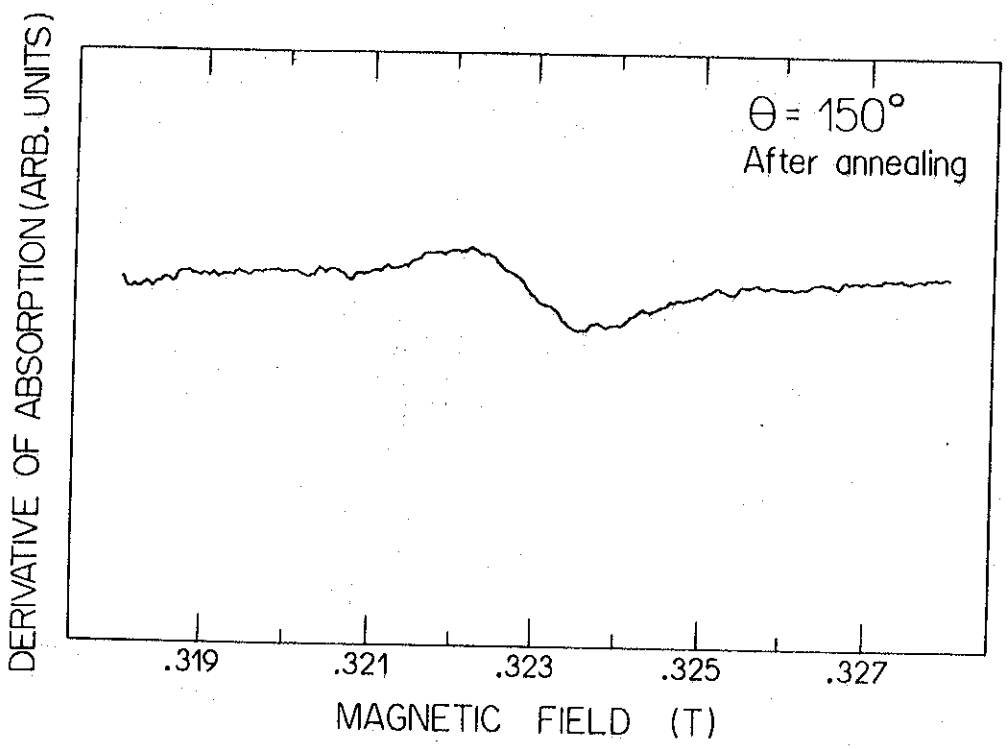
DERIVATIVE OF ABSORPTION (ARB. UNITS)
Θ = 150°
After annealing
.319
.321
.323
.325
.327
MAGNETIC FIELD (T)

Figure 7